



HAL
open science

2D simulation of active species and ozone production in a multi-tip DC air corona discharge

M. Meziane, Olivier Eichwald, J.-P. Sarrette, Olivier Ducasse, Mohammed Yousfi

► **To cite this version:**

M. Meziane, Olivier Eichwald, J.-P. Sarrette, Olivier Ducasse, Mohammed Yousfi. 2D simulation of active species and ozone production in a multi-tip DC air corona discharge. *European Physical Journal: Applied Physics*, 2011, 56 (2), pp.24005. 10.1051/epjap/2011110154 . hal-00746202

HAL Id: hal-00746202

<https://hal.science/hal-00746202>

Submitted on 28 Oct 2012

HAL is a multi-disciplinary open access archive for the deposit and dissemination of scientific research documents, whether they are published or not. The documents may come from teaching and research institutions in France or abroad, or from public or private research centers.

L'archive ouverte pluridisciplinaire **HAL**, est destinée au dépôt et à la diffusion de documents scientifiques de niveau recherche, publiés ou non, émanant des établissements d'enseignement et de recherche français ou étrangers, des laboratoires publics ou privés.

2D SIMULATION OF ACTIVE SPECIES AND OZONE PRODUCTION IN A MULTI-TIP DC AIR CORONA DISCHARGE

M. Meziane, O. Eichwald*, J.P. Sarrette, O. Ducasse, M. Youfii

Université de Toulouse, LAPLACE, UMR du CNRS no. 5213, 118 Route de Narbonne, Bât. 3R2, 31062 Toulouse Cedex 9, France

*Email : eichwald@laplace.univ-tlse.fr

Abstract: The present paper shows for the first time in the literature a complete 2D simulation of the ozone production in a DC positive multi-tip to plane corona discharge reactor crossed by a dry air flow at atmospheric pressure. The simulation is undertaken until 1ms and involves tens successive discharge and post-discharge phases. The air flow is stressed by several monofilament corona discharges generated by a maximum of four anodic tips distributed along the reactor. The non stationary hydrodynamics model for reactive gas mixture is solved using the commercial FLUENT software. During each discharge phase, thermal and vibrational energies as well as densities of radical and metastable excited species are locally injected as source terms in the gas medium surrounding each tip. The chosen chemical model involves 10 neutral species reacting following 24 reactions. The obtained results allow us to follow the cartography of the temperature and the ozone production inside the corona reactor as a function of the number of high voltage anodic tips.

1 Introduction

Non-thermal plasmas created by atmospheric pressure corona discharges are very efficient sources of active species like radicals or excited species. They are therefore used in many applications where chemical activation is needed such as flue gas pollution control [1-2], plasma ignition [3], bio-decontamination [4], medical treatment [5] or ozone production [6]. In this paper, we focus our study on ozone production by multi-points corona discharge. In such device, ozone is produced through the radical O that is created in time laps of about hundred of nanoseconds inside filamentary discharges. These radicals are then transported in the air flow and diffuse in the reactor volume where they interact more particularly with the background O₂ molecules to form O₃. In the present paper we have developed a 2D simulation of these processes by coupling ten discharge / post-discharge phases until 1ms in a reactor having up to four anodic tips. Even if some previous works were already devoted to this kind of simulation [7-8], a complete 2D simulation simultaneously coupling all the energetic, chemical and hydrodynamics phenomena that take place inside a multi-tip corona reactor was never done. This perspective is yet possible because recent works have shown the

ability of the commercial FLUENT software to follow the discharge and post-discharge phases in a mono-tip to plane configuration [9-10]. Section 2 details the used model and the main assumptions. Section 3 describes the simulation conditions and is followed by the description and the analysis of the obtained results.

2 Hydrodynamics model of the discharge and post-discharge phases

The hydrodynamics model is based on the system of non stationary Navier-Stokes equations for reactive gas mixture. It takes into account the conservation equations of mass, momentum, energy and density of each chemical species i , coupled with the conservation equation of the vibrational relaxation energy:

$$\frac{\partial \rho}{\partial t} + \vec{\nabla} \cdot \rho \vec{v} = 0 \quad (1)$$

$$\frac{\partial \rho \vec{v}}{\partial t} + \vec{\nabla} \cdot \rho \vec{v} \vec{v} = -\vec{\nabla} P - \vec{\nabla} \cdot \vec{\tau} \quad (2)$$

$$\frac{\partial \rho m_i}{\partial t} + \vec{\nabla} \cdot \rho m_i \vec{v} + \vec{\nabla} \cdot \vec{J}_i = S_i \quad \forall i \quad (3)$$

$$\frac{\partial \rho h}{\partial t} + \vec{\nabla} \cdot \rho h \vec{v} = \vec{\nabla} \cdot (k \vec{\nabla} T) + \frac{\partial P}{\partial t}$$

$$+ \vec{v} \cdot \vec{\nabla} P + \vec{\tau} : \vec{\nabla} \vec{v} - \vec{\nabla} \cdot \sum_i \vec{J}_i h_i + f_i \vec{j} \cdot \vec{E} + \frac{\varepsilon_v}{\tau_v} \quad (4)$$

$$\frac{\partial \varepsilon_v}{\partial t} + \vec{\nabla} \cdot \varepsilon_v \vec{v} = f_v \vec{j} \cdot \vec{E} - \frac{\varepsilon_v}{\tau_v} \quad (5)$$

ρ is the mass density of the gas, \vec{v} the velocity, P the static pressure and $\vec{\tau}$ the stress tensor. For each chemical species i , n_i and m_i are the density and the mass fraction, \vec{J}_i the diffusive flux due to concentration and thermal gradients, S_i the net rate of production per unit volume (due to chemical reactions). h is the static enthalpy, T the temperature, k the thermal conductivity and ε_v the vibrational energy. f_i and f_v are the fraction of the electron power $\vec{j} \cdot \vec{E}$ transferred into thermal and vibrational energy. In the present study we assumed that the translational, rotational and electronic excitation energies relax immediately and that the vibrational energy stored during the discharge phases relaxes after a mean delay time $\tau_v = 50 \mu s$ [11]. During each discharge phase, we inject inside the discharge volume, the radical and metastable source terms as well as the energetic source terms $f_i \vec{j} \cdot \vec{E}$ and $f_v \vec{j} \cdot \vec{E}$. The magnitude and the profile of the corresponding source terms are taken from a complete corona discharge simulation involving the primary and the secondary streamer propagation [12]. The magnitude and profile of the energetic source terms are taken after the pressure wave initiated by the first thermal shock [13].

3 Simulation conditions

The previous hydrodynamic model is solved using the commercial FLUENT Code. The 2D Cartesian computational domain is displayed in figure 1. It represents a ($2cm \times 1cm$) tip-to-plane corona discharge reactor crossed by a lateral atmospheric air flow of $5ms^{-1}$ at 300K. A maximum of four tips can be used, distant from each other by 5mm. At each tip, a positive DC high voltage of magnitude equal to 7.2kV is applied. Under these conditions, the discharge phase duration is of around 150ns and the natural repetition rate of the discharge is of about 10kHz [12]. The density and energetic source terms profile and magnitude are calculated from a complete simulation of the discharge phase using an optimized 2D streamer corona discharge model

[12]. The simulation involves 10 neutral chemical species (N, O, O₃, NO₂, NO, O₂, N₂, N₂ ($A^3\Sigma_u^+$), N₂ ($a^1\Sigma_u^-$) and O₂ ($a^1\Delta_g$)) reacting following 24 selected chemical reactions. Other species (eg, N₂O, NO₃, etc.) have not been considered in this simulation because of their low concentration in the ionized channel [8]. During each discharge phase, metastable excited species (N₂($A^3\Sigma_u^+$), N₂($a^1\Sigma_u^-$) and O₂($a^1\Delta_g$)), radicals (N and O) and electronic energy are injected for each tip inside a mono-filamentary channel of 50 μm of diameter and located in the gap space between the powered tip and the grounded plan.

4 Results and discussion

Figure 2 shows the cartography of the temperature at 150ns just after the first discharge phase when the four points are stressed by the DC high voltage. As in previous works [9], the temperature increase is confined inside the mono-filamentary discharge zones. The direct relaxation of the translational, rotational and excited energies (modeled by $f_i \vec{j} \cdot \vec{E}$ term in equation (4)) induces a maximum temperature increase of 1200K just around the anodic tips.

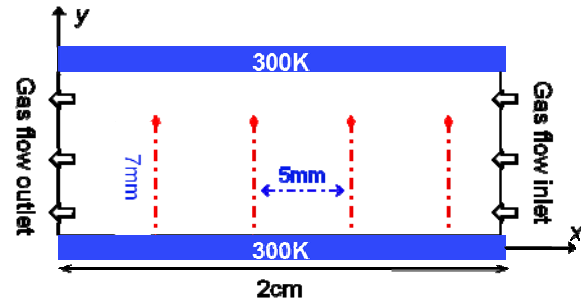


Figure 1: 2D Cartesian simulation domain of the multi-tip to plane corona discharge reactor.

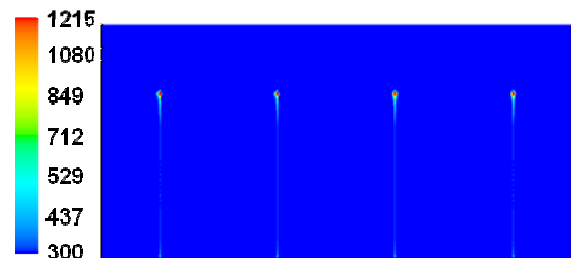


Figure 2: Temperature profile after the first discharge phase at $t = 150ns$.

Figures 3 and 4 show the cartography of the temperature and of the ozone density after 1ms (i.e after 10 discharge and post-discharge phases) when

one, two, three or four tips are stressed by the DC high voltage. Figures 3a and 4a show that for the mono tip case, the lateral air flow and the memory effect of the previous ten discharges leads to a wreath shape of the space distribution of the temperature and the ozone density. The temperature and the ozone maps are very similar. Indeed, both radical and energy source terms are higher near the tip (i.e. inside the secondary streamer area expansion [12]) and near the plane. Furthermore, the production of ozone is obviously sensitive to the gas temperature diminution since it is mainly created by the three body reaction $O + O_2 + M \rightarrow O_3 + M$ (having a reaction rate inversely proportional to gas temperature). For more than one tip, the temperature and ozone wreaths interact each other and their superposition induces locally a rise of both the gas temperature and ozone density (see figures 3 and 4). The local maximum of temperature is of around 325K for one tip case and increases up to 350K for four anodic tips.

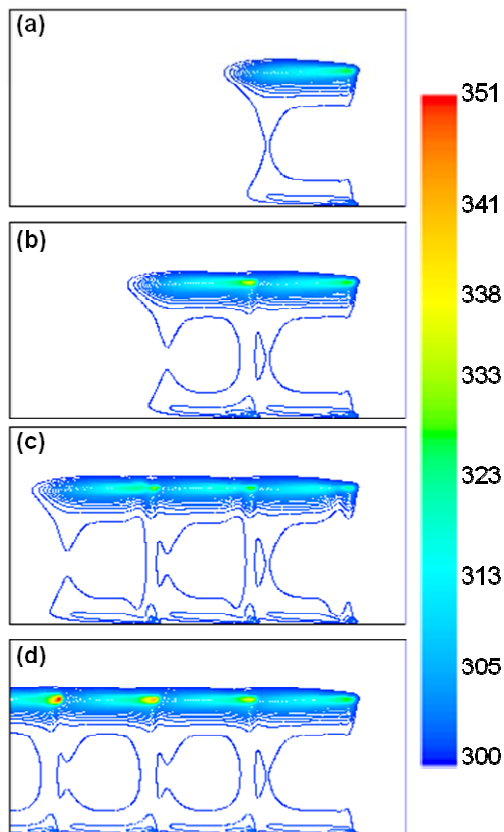


Figure 3: Temperature contours at 1ms i.e. after ten discharge and post-discharge phases. The number of high voltage tip is respectively (a) one, (b) two, (c) three and (d) four.

The average temperature in the whole computational domain remains quasi constant and

the small variations show a linear behavior with the number of anodic tips (see figure 5). A linear increase with proportionality between the ozone density and the number of tips is also observed in figure 6. After 1ms, and for the four tips case, the mean ozone density inside the computational domain reaches $4 \times 10^{14} \text{ cm}^{-3}$. At the end of each discharge phase, the maximum of O radical production is located around the tip and reach about 10^{17} cm^{-3} . We note that the atomic oxygen density decreases with the gas temperature to form ozone, and its population at 1ms is concentrated in the surrounding of each tip, with significant quantity of a 10^{15} cm^{-3} in the reactor (see figure 7).

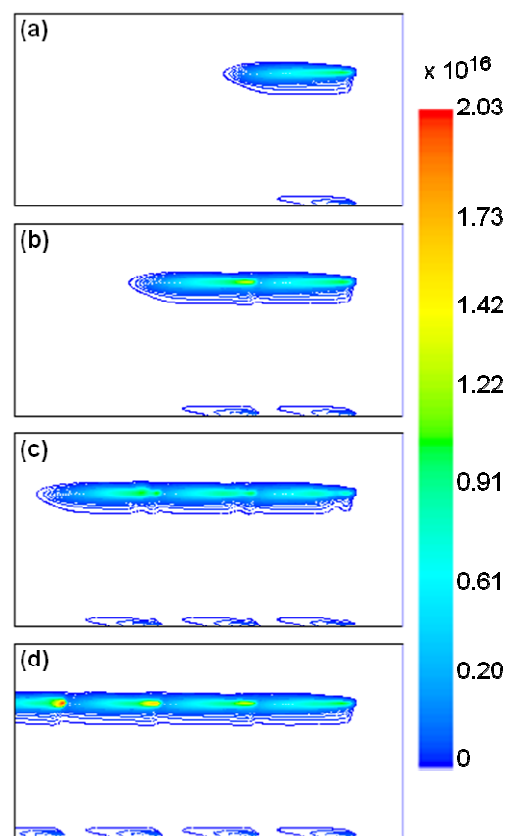


Figure 4: Ozone density contours (cm^{-3}) at 1ms i.e. after ten discharge and post-discharge phases. The number of high voltage tip is respectively (a) one, (b) two, (c) three and (d) four.

Finally, in our simulation conditions, the energy injected per tip after 1ms is of around 0.1mJ. The mean quantity of O_3 created after 1ms and for 1 tip is of around 1.610^{-9} g . Thus the production yield per tip can be estimated of around $16 \mu\text{gJ}^{-1}$ (i.e. $\sim 57 \text{ kWh}^{-1}$) which in accordance with previous experimental work [[6]

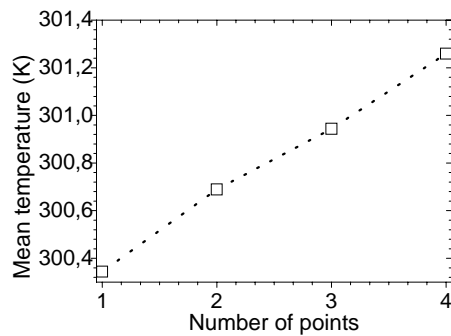


Figure 5: Mean temperature increase inside the computational domain of figure 1 as a function of the number of tips

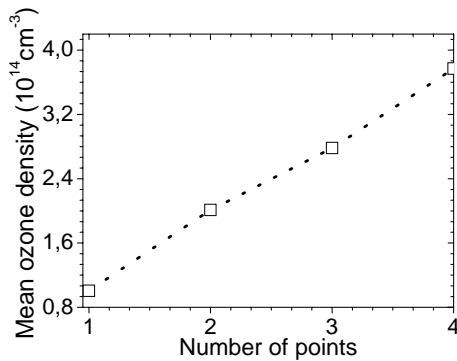


Figure 6: Mean ozone density increase inside the computational domain of figure 1 as a function of the number of tips.

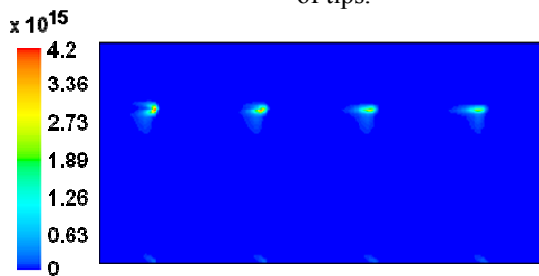


Figure 7: Atomic oxygen density profile (cm^{-3}) at 1ms, i.e. after ten discharge and post-discharge phases, in the case of four anodic tips.

5 Conclusion

The present work shows that the FLUENT software can be used to simulate in details the spatiotemporal evolution of an air flow stressed by repetitive corona discharges under mono and multi-tip anodic electrode configuration. In our simulation conditions, the 2D results show the strong correlation between the temperature decrease and the ozone production. As the O radical density and electronic energy are mainly deposited around the tips during the discharge phases, and because of the lateral air wind, both temperature and ozone concentration increase in a lateral wreath located near the tips and extending

along the whole computational domain. Until 1ms and a maximum of four tips, the mean ozone production is proportional to the number of tips. Finally, one can notice that the complete simulation until 1ms and with four tips needs about 10 days of CPU time on the Hyperion machine [14].

Acknowledgments:

This work was performed using HPC resources from CALMIP (Grant 2011- [P1053]) [14].

References:

1. C Gentile and M J Kushner, *J. Appl. Phys.* (1996) 79 (8).
2. O Eichwald, M Yousfi, A Hennad, M Benabdessadok, *J. Appl. Phys.* (1997) 82 4781.
3. S M Starikovskaia, *J. Phys. D: Appl. Phys.* (2006), 39 R265-R299.
4. JP Sarrette, S Cousty, N Merbahi, A Nègre-Salvayre and F Clement, *Eur. Phys. J. Appl. Phys.* (2010), 49 13108.
5. M Laroussi, A Fridman, P Favia, M R Wertheimer, *Plasma Process. Polym.*, (2010), 7, 193.
6. R Ono and T Oda, *J. Phys. D: Appl. Phys.* (2004) 37 730–5.
7. R Dorai and M J Kushner, *J. Phys. D: Appl. Phys.* (2003) 36 1075–1083.
8. O Eichwald, N A Guntoro, M Yousfi and M Benhenni, *J. Phys. D: Appl. Phys.* (2002), 35 439-450.
9. M Meziane, JP Sarrette, O Eichwald, O Ducasse, M Yousfi, XVIII GD2010, Greifswald, (2010) p.392- 395. M Meziane, JP Sarrette, O Eichwald, O Ducasse, M Yousfi, (to be published).
10. J Batina, F Noel, S Lachaud, R Peyroux and J F Loiseau, *J. Phys. D: Appl. Phys.* (2001), 34 1510 1524.
11. Creighton Y L M 1994 Thesis Eindhoven, Nugi 812.
12. O Eichwald, O Ducasse, D Dubois, A Abahazem, N Merbahi, M Benhenni and M Yousfi, *J. Phys. D: Appl. Phys.* (2008) 41 234002.
13. S Kacem, O Ducasse, H Bensaad, O Eichwald, M Yousfi, K Charrada, XVIII GD2010, Greifswald, (2010) p.276-279.
14. www.calmip.cict.fr/spip/spip.php?rubrique90